ELSEVIER

Ceramics International 29 (2003) 279–285

CERAMICS INTERNATIONAL

www.elsevier.com/locate/ceramint

An analysis of unsteady thermal stresses in a functionally gradient ceramic plate with symmetrical structure

Zhao Jun*, Ai Xing, Huang Chuanzhen, Zhang Jianhua, Deng Jianxin

School of Mechanical Engineering, Shandong University, Jinan 250061, PR China

Received 30 January 2002; received in revised form 12 March 2002; accepted 8 May 2002

Abstract

The analytical formulae of one-dimensional unsteady temperature field and unsteady thermal stress field for a functionally gradient material plate with symmetrical structure were derived by using perturbation method, by which the unsteady temperature fields and unsteady thermal stress fields of an Al_2O_3/(W,Ti)C functionally gradient ceramic plate with symmetrical structure were calculated in case of both surface cooling and surface heating. The results obtained showed that the absolute values of thermal stresses of the functionally gradient ceramic plate are lower than those of the homogeneous ceramic plate for both surface cooling and surface heating cases. Hence an approach to improving the thermal shock resistance of ceramic tool materials i.e. using functionally gradient ceramic tool materials, was put forward and verified by intermittent turning of hardened tool steel.

Keywords: C. Thermal shock resistance; Functionally gradient materials; Heat transfer; Thermal stress; Compositional distribution

1. Introduction

As cutting tool materials, ceramics posses high hardness, wear resistance, heat resistance and chemical stability, with less deformation or dissolution wear in cutting processes. In spite of the advances in strengthening and toughening of ceramic tool materials as well as the improved processing techniques, their applications in intermittent cutting operations are restricted by their intrinsic drawbacks. Due to the lower thermal conductivity, higher thermal expansion coefficient and hence the lower thermal shock resistance, severe temperature gradients and thermal stress gradients are present in the interior of the ceramic cutting tool under cyclic mechanical and thermal shock in an intermittent cutting process, which may lead to the fracture of the cutting edge. Unpredictable failure by fracture can lead to damage to the part being machined or to the machine tool, both of which can be several orders of magnitude more valuable than the tool itself in modern industry with the increased use of CNC machine tools.

The introduction of the concept of functionally gradient materials (FGM) into the fabrication of ceramic cutting tool materials provided an approach to improving their thermal and mechanical properties [1,2]. If we design and fabricate the ceramic tool material with compositional distribution, microstructure varying continuously along the thickness direction in an appropriate way to achieve the improved thermal and mechanical properties especially thermal shock resistance to meet the critical requirements of cutting process, it is expected to improve the fracture resistance especially the thermal fracture resistance of ceramic tool materials.

Based on the deep understanding of the working conditions for ceramic tools, a design model for functionally gradient ceramic tool materials with symmetrical composition distribution was developed by the author [1,2]. In the present paper, the analytical formulae of one-dimensional unsteady temperature field and unsteady thermal stress field for a functionally gradient material plate with symmetrical structure were derived by using perturbation method, by which the unsteady temperature fields and unsteady thermal stress fields of an Al_2O_3/(W,Ti)C functionally gradient ceramic plate with symmetrical structure were calculated in

* Corresponding author. Tel.: +86-531-8393904; fax: +86-531-8392618.

E-mail address: zhaojun@sdu.edu.cn (J. Zhao).

0272-8842/03/$22.00
PII: S0272-8842(02)00116-5

case of both surface cooling and surface heating. The influence of the compositional distribution of functionally gradient ceramic materials on thermal stresses were examined, according to which a method of improving the thermal shock resistance of ceramic tool materials i.e. using functionally gradient ceramic tool materials, was put forward and verified by intermittent turning tests.

2. Analytical development

As shown in Fig. 1 a, consider an infinite functionally gradient ceramic plate with symmetrical structure with its thickness being $2r_m$. It is assumed that initially the medium is at the uniform temperature T_0 and is suddenly subjected to an uniform temperature T_s by the surrounding medium, so the thermal loading conditions are also symmetrical.

The thermo-mechanical properties of the plate are all varied in the thickness direction continuously. Hence the temperature field and thermal stress field are also functions of position z. From the symmetrical structure and symmetrical thermal loading conditions, it is reasonable to simplify the model into the form shown in Fig. 1b with only the upper half being studied.

The one-dimensional heat conduction equation of nonhomogeneous solids for a transient state [3], the initial and thermal boundary conditions are given as follows

$$c(z)\rho(z)\frac{\partial T}{\partial t}=\frac{\partial}{\partial z}\left[k(z)\frac{\partial T}{\partial z}\right] \tag{1}$$

$$t=0;\ T=T_0 \tag{2}$$

$$\left.\begin{array}{l} z=0;\ \dfrac{\mathrm{d}T}{\mathrm{d}z}=0 \\ z=r_m;\ T=T_s \end{array}\right\} \tag{3}$$

where T is temperature, t is time, z is the coordinate variable in the thickness direction, and $c(z)$, $\rho(z)$, $k(z)$ are specific heat, specific gravity and thermal conductivity respectively. For the purpose of simplicity, the following dimensionless variables are introduced:

$$U=\frac{T-T_0}{T_s-T_0}=\frac{T-T_0}{\Delta T}$$

$$\hat{z}=\frac{z}{r_m},\ \hat{c}(\hat{z})=\frac{c(\hat{z})}{c_0}$$

$$\hat{\rho}(\hat{z})=\frac{\rho(\hat{z})}{\rho_0},\ \hat{k}(\hat{z})=\frac{k(\hat{z})}{k_0} \tag{4}$$

where c_0, ρ_0 and k_0 are specific heat, specific gravity and thermal conductivity of the upper boundary ($\hat{z}=1$). According to heat transfer, the thermal diffusivity of the upper boundary is:

$$a_0=\frac{k_0}{c_0\rho_0} \tag{5}$$

Hence, the dimensionless time can be given as:

$$\tau=\frac{a_0}{r_m^2}t \tag{6}$$

By referring to Eqs. (4) and (6), the heat conduction Eq. (1) has the following dimensionless form:

$$\hat{c}(\hat{z})\hat{\rho}(\hat{z})\frac{\partial U}{\partial \tau}=\frac{\partial}{\partial \hat{z}}\left[\hat{k}(\hat{z})\frac{\partial U}{\partial \hat{z}}\right] \tag{7}$$

Because $\hat{c}(\hat{z})$, $\hat{\rho}(\hat{z})$, $\hat{k}(\hat{z})$ are all variables, the partial differential equation in the form of Eq. (7) can not be solved. We introduce a new variable η:

$$\eta=\int_0^{\hat{z}}\frac{1}{\sqrt{\hat{a}(\hat{z})}}d\hat{z} \tag{8}$$

where $\hat{a}(\hat{z})=\dfrac{\hat{k}(\hat{z})}{\hat{c}(\hat{z})\hat{\rho}(\hat{z})}$

Thereafter the heat conduction equation, the initial and thermal boundary conditions become:

$$\frac{\partial^2 U}{\partial \eta^2}+\frac{\partial}{\partial \eta}\ln\sqrt{\hat{c}(\eta)\hat{\rho}(\eta)\hat{k}(\eta)}\frac{\partial U}{\partial \eta}=\frac{\partial U}{\partial \tau} \tag{9}$$

$$\tau=0;\ U=0 \tag{10}$$

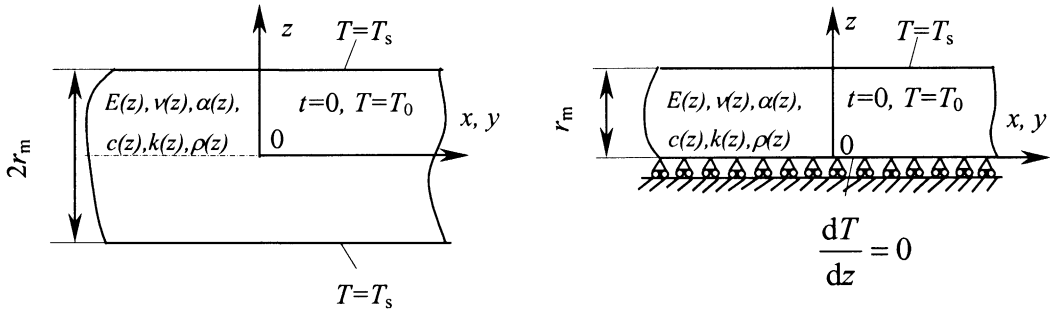

Fig. 1. Functionally gradient ceramic plate with symmetrical structure.

$$\left.\begin{array}{l}\eta=0;\ \dfrac{\mathrm{d}U}{\mathrm{d}\eta}=0\\ \eta=\int_0^1\dfrac{1}{\sqrt{\hat{a}}}d\hat{z}=\zeta;\ U=1\end{array}\right\} \tag{11}$$

where ζ is a constant for a functionally gradient ceramic plate with given compositional distribution.

By applying the Laplace transform to Eq. (9), we obtain:

$$\frac{\mathrm{d}^2U^*}{\mathrm{d}\eta^2}+\frac{\mathrm{d}}{\mathrm{d}\eta}\ln\sqrt{\hat{c}(\eta)\hat{\rho}(\eta)\hat{k}(\eta)}\frac{\mathrm{d}U^*}{\mathrm{d}\eta}-sU^*=-U_0 \tag{12}$$

In order to solve Eq. (12) by using perturbation method, we ask:

$$\frac{\mathrm{d}}{\mathrm{d}\eta}\ln\sqrt{\hat{c}(\eta)\hat{\rho}(\eta)\hat{k}(\eta)}=\delta\phi(\eta) \tag{13}$$

where δ is a very small parameter. Eq. (12) becomes:

$$\frac{\mathrm{d}^2U^*}{\mathrm{d}\eta^2}+\delta\phi\frac{\mathrm{d}U^*}{\mathrm{d}\eta}-sU^*=-U_0 \tag{14}$$

Eq. (14) has the perturbation solution of the following form:

$$U^*=\sum_{i=0}^{\infty}\delta^iU^{*(i)} \tag{15}$$

So Eq. (14) becomes:

$$\frac{\mathrm{d}^2U^{*(0)}}{\mathrm{d}\eta^2}-sU^{*(0)}=-U_0;\ i=0 \tag{16}$$

and

$$\frac{\mathrm{d}^2U^{*(i)}}{\mathrm{d}\eta^2}-sU^{*(i)}=-\phi\frac{\mathrm{d}U^{*(i-1)}}{\mathrm{d}\eta};\ i\geqslant 1 \tag{17}$$

The solutions of Eqs. (16) and (17) can be expressed as:

$$U^{*(0)}=A_0\mathrm{ch}\sqrt{s}\eta+B_0\mathrm{sh}\sqrt{s}\eta-\frac{1}{\sqrt{s}}\int_0^{\eta}U_0\mathrm{sh}\sqrt{s}(\eta-\xi)\mathrm{d}\xi \tag{18}$$

and

$$U^{*(i)}=A_i\mathrm{ch}\sqrt{s}\eta+B_i\mathrm{sh}\sqrt{s}\eta-\frac{1}{\sqrt{s}}\int_0^{\eta}\phi\frac{\mathrm{d}U^{*(i-1)}}{\mathrm{d}\xi}\mathrm{sh}\sqrt{s}(\eta-\xi)\mathrm{d}\xi \tag{19}$$

where unknown coefficients A_0, B_0, A_i and B_i can be obtained by using the boundary conditions.

By applying the Laplace transform to Eq. (11), the boundary conditions in the s-plane are:

$$\left.\begin{array}{l}\eta=0;\dfrac{\mathrm{d}U^{*(0)}}{\mathrm{d}\eta}=0\\ \eta=\zeta;\ U^{*(0)}=1/s\end{array}\right\};\ i=0 \tag{20}$$

and

$$\left.\begin{array}{l}\eta=0;\ U^{*(i)}=0\\ \eta=\zeta;\ U^{*(i)}=0\end{array}\right\};\ i\geqslant 1 \tag{21}$$

From Eqs. (18) and (20), we have:

$$U^{*(0)}=\frac{\mathrm{ch}\sqrt{s}\eta}{s\mathrm{ch}\sqrt{s}\zeta} \tag{22}$$

By substituting Eqs. (22) and (21) into Eq. (19), we can obtain A_1, B_1 and

$$\delta U^{*(1)}=\frac{\mathrm{sh}\sqrt{s}\eta}{\sqrt{s}\mathrm{sh}\sqrt{s}\zeta\mathrm{ch}\sqrt{s}\zeta}\int_0^{\zeta}\ln\sqrt{\hat{c}\hat{\rho}\hat{k}}\mathrm{sh}\sqrt{s}(\zeta-2\xi)\mathrm{d}\xi-\frac{1}{\sqrt{s}\mathrm{ch}\sqrt{s}\zeta}\int_0^{\eta}\ln\sqrt{\hat{c}\hat{\rho}\hat{k}}\mathrm{sh}\sqrt{s}(\eta-2\xi)\mathrm{d}\xi \tag{23}$$

Terms $\delta^2U^{*(2)}$, $\delta^3U^{*(3)}$...can also be obtained by means of the iterative computations.

By applying inverse Laplace transform to Eqs. (22) and (23), respectively, we have:

$$U^{(0)}=1+\sum_{j=0}^{\infty}\frac{4}{(2j+1)\pi}(-1)^{j+1}\cos\frac{2j+1}{2\zeta}\eta\pi\exp\left[-\left(\frac{2j+1}{2\zeta}\pi\right)^2\tau\right] \tag{24}$$

and

$$\begin{aligned}\delta U^{(1)}=&\frac{2}{\zeta}\sum_{j=1}^{\infty}(-1)^j\exp\left[-\left(\frac{j\pi}{\zeta}\right)^2\tau\right]\sin\frac{j\eta}{\zeta}\pi\\&\times\int_0^{\zeta}\ln\sqrt{\hat{c}\hat{\rho}\hat{k}}\sin\frac{2j\xi}{\zeta}\pi\ \mathrm{d}\xi\\&+\frac{2}{\zeta}\sum_{j=0}^{\infty}(-1)^j\exp\left[-\left(\frac{2j+1}{2\zeta}\pi\right)^2\tau\right]\\&\times\left\{\sin\frac{2j+1}{2\zeta}\eta\pi\left[\int_0^{\zeta}\ln\sqrt{\hat{c}\hat{\rho}\hat{k}}\cos\frac{2j+1}{\zeta}\xi\pi\ \mathrm{d}\xi-\int_0^{\eta}\ln\sqrt{\hat{c}\hat{\rho}\hat{k}}\cos\frac{2j+1}{\zeta}\xi\pi\ \mathrm{d}\xi\right]\right.\\&\left.+\cos\frac{2j+1}{2\zeta}\eta\pi\int_0^{\eta}\ln\sqrt{\hat{c}\hat{\rho}\hat{k}}\sin\frac{2j+1}{\zeta}\xi\pi\ \mathrm{d}\xi\right\}\end{aligned} \tag{25}$$

We can obtain the unsteady temperature field $U(\eta, \tau)$, $U(\hat{z}, \tau)$ and $T(\hat{z}, \tau)$ after the terms $\delta^2 U^{(2)}$, $\delta^3 U^{(3)}$...are calculated by applying inverse Laplace transform to $\delta^2 U^{*(2)}$, $\delta^3 U^{*(3)}$....

Because of the symmetry of both the structure and the thermal loading conditions, the functionally gradient ceramic plate is expansion and contraction unconstrained and bending constrained during the thermal shock process as shown in Fig. 1b, so the thermal stress in z direction (σ_z) is zero. According to Hooke's law and by referring to Eq. (4), the unsteady thermal stress $\sigma(\hat{z}, \tau)$ can be expressed as:

$$\begin{aligned}\sigma(\hat{z}, \tau) &= \sigma_x(\hat{z}, \tau) = \sigma_y(\hat{z}, \tau) \\ &= \frac{E(\hat{z})}{1-\nu(\hat{z})}\left\{\varepsilon(\hat{z}, \tau) - \alpha(\hat{z})[T(\hat{z}, \tau) - T_0]\right\} \\ &= \frac{E(\hat{z})}{1-\nu(\hat{z})}[\varepsilon(\tau) - \alpha(\hat{z})\cdot\Delta T\cdot U(\hat{z}, \tau)] \end{aligned} \tag{26}$$

where $\varepsilon(\tau)$ is the strain of the plate.

The mechanical boundary condition is:

$$\int_0^1 \sigma(\hat{z}, \tau)\mathrm{d}\hat{z} = 0 \tag{27}$$

By substituting Eq. (26) into (27), we have:

$$\varepsilon(\tau) = \Delta T\frac{\int_0^1 E^*(\hat{z})\alpha(\hat{z})U(\hat{z}, \tau)\mathrm{d}\hat{z}}{\int_0^1 E^*(\hat{z})\mathrm{d}\hat{z}} \tag{28}$$

where $E^*(\hat{z}) = \frac{E(\hat{z})}{1-\nu(\hat{z})}$

Hence the unsteady thermal stress $\sigma(\hat{z}, \tau)$ can be obtained by substituting Eq. (28) into (26).

3. Calculations of unsteady thermal stresses

3.1. Compositional distribution of functionally gradient ceramic material

We consider Al_2O_3/(W,Ti)C functionally gradient ceramic plate for the numerical calculations. By not taking into account pores and other very small amounts of additives, the volume fraction of (W,Ti)C along the thickness direction ($\hat{z}$ direction) is of the following exponential form [1,2] (Fig. 2):

$$\varphi_{(W,Ti)C}(\hat{z}) = \begin{cases} (\varphi_1 - \varphi_0)(-\hat{z})^n + \varphi_0 & -1 \leqslant \hat{z} \leqslant 0 \\ (\varphi_1 - \varphi_0)\hat{z}^n + \varphi_0 & 0 \leqslant \hat{z} \leqslant 1 \end{cases} \tag{29}$$

where n is the distribution exponent which determine the compositional distribution of the material, φ_1 and φ_0 are volume fractions of (W,Ti)C of two surfaces ($\hat{z} = \pm 1.0$) and the middle position ($\hat{z} = 0$) respectively.

Data of the physical properties of Al_2O_3 and (W,Ti)C are listed in Table 1. Young's modulus E and Poisson's ratio ν of Al_2O_3/(W,Ti)C composites with different mixture ratios were obtained by Mori-Tanaka's equation [4], thermal expansion coefficients α of different composites were calculated by using Kerner's equation [5], and thermal conductivities k and specific heats c were obtained by the theory of Kingery [6].

The volume fractions of (W,Ti)C φ_1 and φ_0 were assigned as 45 and 30%, respectively. So the thermal expansion coefficient of the material increases from the surface to the middle position continuously (referring to Table 1). This may lead to the formation of residual compressive stresses in the surface region of the compact during the fabricating process (cooling from the sintering temperature to room temperature), which is favourable for an insert made of this material to resist external loading in cutting process. We take the distribution exponent n as 1.2 for the numerical calculation of transient thermal stress field, which was determined with the aim of the highest structural integrity of the compact i.e. the lowest residual thermal stress (Von Mises stress calculated by means of finite element method) in fabricating process. However, the details are omitted here for brevity.

3.2. Numerical results

The dimensionless temperature distribution and the temperature distribution under surface cooling (initial temperature $T_0 = 300$ °C and ambient temperature $T_s = 20$ °C) are shown in Figs. 3 and 4. It can be seen that the shorter the dimensionless time τ is, the higher the temperature gradient near the surface is; the longer τ

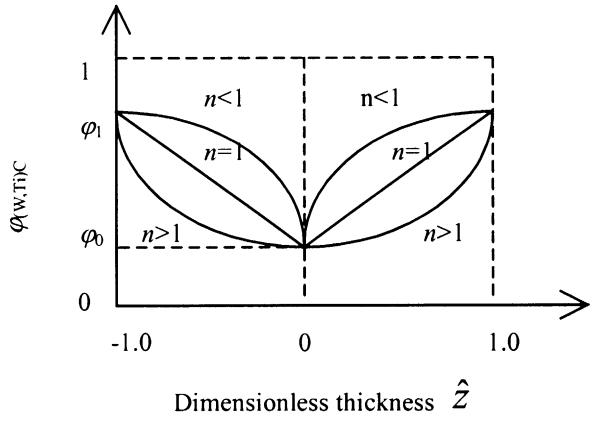

Fig. 2. Symmetrical composition distribution.

Table 1
Data of the physical properties of Al_2O_3 and (W,Ti)C

Materials	Specific gravity ρ/gcm^{-3}	Thermal conductivity (20 °C)k/W(mK)$^{-1}$	Specific heat (20 °C)c/cal(gK)$^{-1}$	Thermal expansion coefficient (20 °C)α/10^{-6}K^{-1}	Young's modulus E/GPa	Poisson's ratio ν
α-Al_2O_3	3.99	40.37	0.185	8.5	380	0.26
(W,Ti)C	9.56	26.74	0.071	5.8	550	0.194

is, the lower the temperature gradient near the surface is. When τ approaches ∞, the functionally gradient ceramic plate exhibits an uniform temperature distribution.

The calculation results of unsteady thermal stress distribution under surface cooling (Fig. 5) revealed clearly that the tensile stress generated in the surface region ($\hat{z} = \pm 1.0$), while the middle region ($\hat{z} = 0$) was subjected to compressive stress when the dimensionless time τ was shorter. It also can be seen that the shorter the dimensionless time τ is, the higher the tensile stress in the surface region is; the longer τ is, the lower the tensile stress is. When the dimensionless time τ approaches ∞, namely at the steady state, the residual compressive stress will generate in the surface region ($\hat{z} = \pm 1.0$), while the residual tensile stress will generate in the middle region ($\hat{z} = 0$) since the thermal expansion coefficient of the surface region is lower than that of the middle region (Table 1).

As shown in Fig. 6, the functionally gradient ceramic plate under surface heating (initial temperature $T_0 = 20$ °C and ambient temperature $T_s = 300$ °C) exhibits an opposite thermal stress distribution to that for surface cooling case, with the equal absolute values of the thermal stresses but reverse attributes (tensile vs. compressive) at same positions ($\hat{z}$).

In order to investigate the influence of compositional distribution on thermal stress distribution, the unsteady thermal stress distribution of a homogeneous Al_2O_3/(W,Ti)C ceramic plate under surface cooling (initial temperature $T_0 = 300$ °C and ambient temperature $T_s = 20$ °C) was calculated by using the same method. The volume fraction of (W,Ti)C for the homogeneous Al_2O_3/(W,Ti)C ceramic plate is 45%, which is equal to that of the surface layer of the functionally gradient ceramic plate. The calculation results for $\tau = 0.1$ are listed in Table 2. It can be seen that the absolute values of both tensile stresses in the surface region and the compressive stresses in the middle region of the homogeneous ceramic plate are higher than those of the gradient ceramic plate. We can find the similar characteristics of the thermal stress distributions for $\tau = 0.01$ and $\tau = 1.0$.

The lower thermal stresses of the functionally gradient ceramic plate should be attributed to both the higher thermal conductivity and the higher thermal

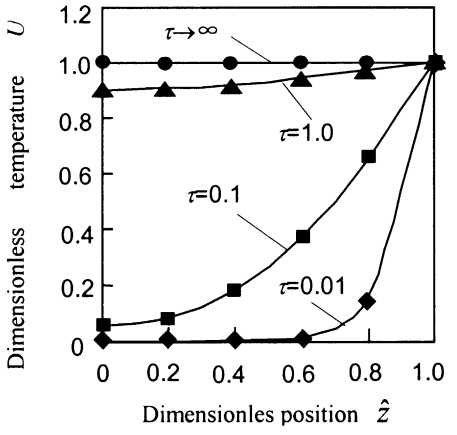

Fig. 3. Dimensionless temperature.

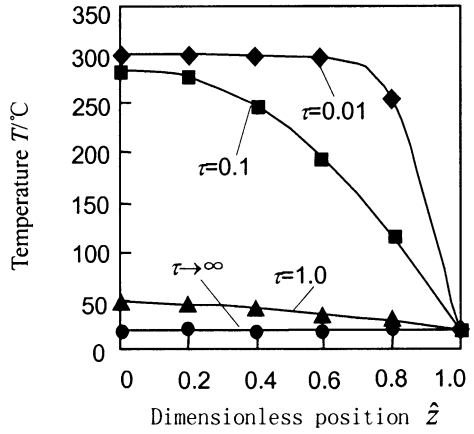

Fig. 4. Temperature distribution under surface cooling.

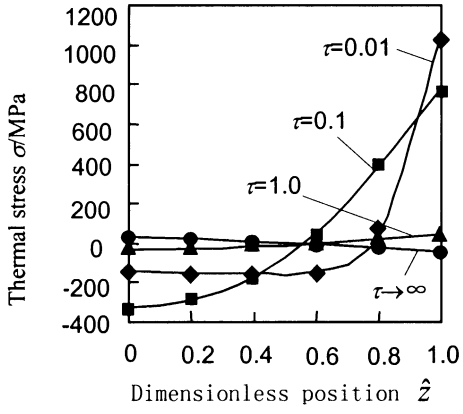

Fig. 5. Thermal stress distribution under surface cooling.

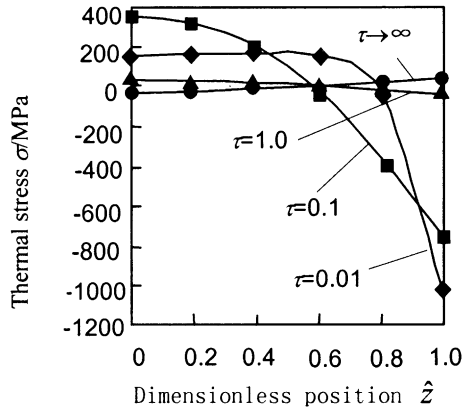

Fig. 6. Thermal stress distribution under surface heating.

expansion coefficient of the middle region than those of the surface region (Table 1). The former could relax the temperature gradient and the later could partially release the tensile stress in the surface region during the cooling process, and the higher the temperature difference ΔT ($=T_s-T_0$) is, the more remarkably the functionally gradient ceramic plate release the thermal stress. Likewise, the absolute values of both the compressive stress in the surface region and the tensile stress in the middle region are lower than those of the homogeneous ceramic plate in case of surface heating.

The lower absolute values of unsteady thermal stresses of functionally gradient ceramic plate than those of the homogeneous ceramic plate are indicative of its better thermal shock behavior than that of homogeneous ceramics.

It can be inferred from the above results that a functionally gradient ceramic tool made in accordance with the above compositional distribution would release the alternating temperature gradient and the thermal stress resulted from the cyclic thermal shock in an intermittent cutting process, and furthermore improve the fracture resistance of ceramic tools.

4. Intermittent cutting tests

According to the pre-determined compositional distribution exponent $n=1.2$ (Fig. 2), an Al_2O_3/(W,Ti)C functionally gradient ceramic tool material FG-2 with symmetrical structure was synthesized by using hot-pressing technique [7]. Its cutting behavior in intermittent turning of hardened carbon tool steel T10A (57–61 HRC) was investigated in comparison with that of a homogeneous Al_2O_3/(W,Ti)C ceramic tool SG-4 [45 vol.%(W,Ti)C]. The machining experiments were carried out on a CA6140 lathe equipped with a 75° lead angle, 10° negative inclination, 10° negative rake tool holder. The geometry of the tool inserts was SNG15083, with an edge chamfer of 0.2 mm at 20°. Four pieces of T10A plates with the thickness of 16 mm were clamped in the four peripheral straight slots of a cylindrical fixture by screws. So the insert will undertake four times of cuts during each revolution of the fixture.

Since tool life is generally dominated by the cutting speed, the cutting experiments were carried out under the cutting speeds $v=100$, 133 and 200 m min^{-1}, with the fixed feed rate of 0.1 mm rev^{-1} at a 0.15 mm depth of cut. Because of the randomness of the fracture of ceramics, the tests were conducted for 10 times under each cutting condition. The data of average tool lives of FG-2 and SG-4 are listed in Table 3, with edge fracture as tool life criterion. Results revealed that the FG-2 tool had less advantage over common ceramic tool SG-4 when machining at a lower cutting speed (100 m min^{-1}). However, the fracture resistance of FG-2 tool was much higher than that of SG-4 tool when machining at higher cutting speeds, with tool life of FG-2 increasing by more than 100% that of SG-4 when machining at $v=200$ m min^{-1}.

Tool fracture is caused by the combined effects of alternating mechanical stresses and thermal stresses in an intermittent cutting process [8]. When machining at lower cutting speeds, tool fracture is caused mainly by the mechanical shock because the cutting temperature is relatively low. The effect of thermal stress relaxation of the functionally gradient ceramic tool is not sufficient, so the two tools present equivalent cutting performances. However, when cutting at a higher speed, the inserts are mainly subjected to the high frequency alternating thermal stresses (alternation of tensile and compressive stresses) caused by the high frequency alternation of cutting and air-cutting (heating and cooling) processes in virtue of the decreased cutting forces and mechanical stresses, so tool life is controlled by fracture resulted from the high frequency alternating thermal stresses. Therefore the higher fracture resistance of the gradient ceramic tool FG-2 than that of SG-4

Table 2
Distribution of thermal stress $\sigma(\hat{z}, \tau)$/MPa under surface cooling for $\tau=0.1$

Materials	$\hat{z}$					
	0.0	0.2	0.4	0.6	0.8	1.0
Functionally gradient ceramic plate	−319.9	−286.5	−169.5	50.4	382.3	783.5
Homogeneous ceramic plate	−324.6	−288.7	−170.4	56.1	389.7	802.7

Table 3
Data of tool lives (number of cuts)

Cutting tools	Cutting speeds (m min^{-1})		
	100	133	200
FG-2	$25\ 668^{+7132}_{-5796}$	$21\ 993^{+6855}_{-7461}$	$12\ 604^{+5296}_{-4932}$
SG-4	$25\ 496^{+8532}_{-9188}$	$13\ 410^{+5538}_{-6270}$	5221^{+2879}_{-2157}

tool should be attributed to the improved thermal shock resistance of FG-2.

5. Conclusions

The analytical formulae of one-dimensional unsteady temperature field and unsteady thermal stress field for a functionally gradient material plate with symmetrical structure were derived by using perturbation method, by which the unsteady temperature fields and unsteady thermal stress fields of an Al_2O_3/(W,Ti)C functionally gradient ceramic plate with symmetrical structure were calculated in case of both surface cooling and surface heating. A method of improving the thermal shock resistance of ceramic tool materials i.e. using functionally gradient ceramic tool materials, was put forward and verified by intermittent turning tests.

(1) The calculation results of thermal stress under surface cooling revealed that the tensile stress generated in the surface region, while the middle region was subjected to compressive stress when the dimensionless time τ was shorter. The shorter the dimensionless time τ is, the higher the tensile stress in the surface region is; the longer τ is, the lower the tensile stress is. When the dimensionless time τ approaches ∞, namely at the steady state, the residual compressive stress will generate in the surface region, while the residual tensile stress will generate in the middle region since the thermal expansion coefficient of the surface region is lower than that of the middle region. The functionally gradient ceramic plate under surface heating exhibits an opposite thermal stress distribution to that for surface cooling case.

(2) In case of both surface cooling and surface heating, the absolute values of thermal stresses of the functionally gradient ceramic plate are always lower than those of the homogeneous ceramic plate, namely the functionally gradient ceramic plate can relax thermal stress, the effect increasing with the increase of the temperature difference.

(3) Results of intermittent cutting of hardened tool steel indicated that the functionally gradient ceramic tool FG-2 had less advantage over common ceramic tool SG-4 when machining at lower cutting speeds. However, the fracture resistance of FG-2 tool was much higher than that of SG-4 tool when machining at higher cutting speeds as a result of its improved thermal shock resistance.

Acknowledgements

This work is supported by the National Natural Science Foundation of China (59505014 and 50105011) and the Research Fund for Outstanding Young Scientists of Shandong Province (97215521).

References

[1] J. Zhao, X. Ai, J.H. Zhang, C.Z. Huang, Design of Al_2O_3/TiC functionally gradient ceramic tool material, Chinese J. Mech. Eng. 34 (4) (1998) 32–36. (in Chinese).
[2] X. Ai, J. Zhao, C.Z. Huang, J.H. Zhang, Development of an advanced ceramic tool material—functionally gradient cutting ceramics, Mater. Sci. Eng. A 248 (1–2) (1998) 125–131.
[3] Y. Obata, N. Noda, Unsteady thermal stresses in a functionally gradient material plate (Analysis of one-dimensional unsteady heat transfer problem), Trans. Jpn. Soc. Mech. Eng. 59 (4) (1993) 208–214, (in Japanese).
[4] T. Mori, K. Tanaka, Average stress in matrix and average elastic energy of materials with misfitting inclusions, Acta Metall. 21 (1973) 571.
[5] E.H. Kerner, The elastic and thermal-elastic properties of composite media, Proc. Phys. Soc. B69 (1956) 808–813.
[6] W.D. Kingery, H.K. Bowen, D.R. Uhlmann, Introduction to Ceramics, 2nd ed, John Wiley & Sons Inc, New York, 1976.
[7] J. Zhao, X. Ai, J.H. Zhang, J.X. Deng, C.Z. Huang, Design and properties of a functionally gradient ceramic tool material, Acta Metall. Sinica (English Letters) 12 (5) (1999) 1054–1058.
[8] X. Al, H. Xiao, Machining with Ceramic Cutting Tools, China Machine Press, Beijing, 1988. (in Chinese).